Constraining new forces in the Casimir regime using the isoelectronic technique

R. S. Decca D. Lopez H. B. Chan

E. Fischbach D. E. Krause C. R. Jamell

Constraining New Forces in the Casimir Regime Using the Isoelectronic Technique

R. S. Decca,[1,*] D. López,[2] H. B. Chan,[3] E. Fischbach,[4] D. E. Krause,[5,4] and C. R. Jamell[1]

[1]*Department of Physics, Indiana University-Purdue University Indianapolis, Indianapolis, Indiana 46202, USA*
[2]*Bell Laboratories, Lucent Technologies, Murray Hill, New Jersey 07974, USA*
[3]*Department of Physics, University of Florida, Gainesville, Florida 32611, USA*
[4]*Department of Physics, Purdue University, West Lafayette, Indiana 47907, USA*
[5]*Physics Department, Wabash College, Crawfordsville, Indiana 47933, USA*

(Received 1 February 2005; published 20 June 2005)

We report the first isoelectronic differential force measurements between an Au-coated probe and two Au-coated films, made out of Au and Ge. These measurements, performed at submicron separations using soft microelectromechanical torsional oscillators, eliminate the need for a detailed understanding of the probe-film Casimir interaction. The observed differential signal is directly converted into limits on the parameters α and λ which characterize Yukawa-like deviations from Newtonian gravity. We find $\alpha \lesssim 10^{12}$ for $\lambda \sim 200$ nm, an improvement of ~ 10 over previous limits.

DOI: 10.1103/PhysRevLett.94.240401 PACS numbers: 03.70.+k, 12.20.Ds, 12.20.Fv, 42.50.Lc

Gravity was the first fundamental force to be understood, but the quest to unify it with the other fundamental forces remains elusive. One of the reasons is the apparent weakness of the gravitational interaction at small separations. Recently, a number of experimental searches for new forces over ultrashort distances has been performed [1–9]. They have been stimulated by at least two different, but related, motivations: (a) unification theories that incorporate n compact extra spatial dimensions (of size R_n) predict deviations from Newtonian gravity over sub-mm scales [10–12]. They are characterized by a potential $V(r) = V_N(r)[1 + \alpha e^{-r/\lambda}]$ [10–12], where $V_N(r)$ is the Newtonian gravitational potential for two point masses separated by a distance $r \gg R_n$, and α and $\lambda \sim R_n$ are constants. Thus, the extra-dimensional theories of Ref. [10] provide, for $n > 1$, a naturally small parameter R_n and an associated constant α_n which is relatively poorly constrained. (b) String theory and other extensions to the standard model predict the existence of new light bosons [11]. Their exchange leads to Yukawa corrections to gravity as in (a) above, with $\alpha \gg 1$ and λ, related to the boson mass m by $\lambda = \hbar/mc$, as large as a few microns.

Consequently, limits on α may provide useful guidance in connecting high energy physics to the standard model. Existing limits on α are relatively weak for several reasons: for small λ, the effective interacting masses are themselves necessarily small, and hence background disturbances play a relatively more important role. For experiments with typical separations $\lesssim 1$ μm, the dominant background arises from the Casimir force [4,13], which is relatively strong over the relevant distances and difficult to completely characterize at the required level of precision [1]. Absent any alternative, limits on $\alpha = \alpha(\lambda)$ have been inferred by developing detailed theoretical models of the Casimir interaction [1], yielding the limit $\alpha \lesssim 10^{13}$ for $\lambda \cong 150$ nm.

In this Letter we experimentally subtract the Casimir background at the outset, thus avoiding the necessity to model the Casimir force. This amounts to a ''Casimir-less'' measurement in the Casimir regime, which is made possible by use of the isoelectronic technique (IET) [3,14]. The IET exploits the essentially electronic nature of the Casimir force, whereas gravity and hypothetical forces couple to both nucleons and electrons. Hence, vacuum fluctuations cannot account for any significant difference in the forces between a probe and two materials with identical electronic properties.

A schematic of our setup is shown in Fig. 1. We compare force *differences* over two dissimilar materials, Au and Ge, which have been coated with a common layer of Au of thickness $d^p_{\mathrm{Au}} > \lambda_p$, where $\lambda_p = 135$ nm is the plasma wavelength for Au. The fractional difference of the Casimir force between two infinitely thick metallic plates and two plates of thickness d^p_{Au} is $\sim e^{-4\pi d^p_{\mathrm{Au}}/\lambda_p} \sim 10^{-6}$ [15]. In our experiment, this translates to a difference $\Delta F_C \lesssim 10^{-17}$ N between the Au-coated sphere and the two sides of the Au/Ge composite sample. Since this force is smaller than the experimental sensitivity, any signal detected as the probe oscillates over the Au/Ge composite sample (which has a large mass density difference, $\rho_{\mathrm{Au}} - \rho_{\mathrm{Ge}} = 13.96 \times 10^3$ kg/m^3) must be due to an interaction via either gravity or some new hypothetical force. Thus, limits on $\alpha(\lambda)$ can be obtained, without having to resort to a theory of the Casimir force. The hypothetical force difference is

$$\begin{aligned} \Delta F_h &= -4\pi^2 G\alpha\lambda^3 e^{-z/\lambda} R K_s K_p, \\ K_s &= [\rho_{\mathrm{Au}} - (\rho_{Au} - \rho_{\mathrm{Cr}})e^{-d^s_{\mathrm{Au}}/\lambda} \\ &\quad - (\rho_{\mathrm{Cr}} - \rho_s)e^{-(d^s_{\mathrm{Au}} + d_{\mathrm{Cr}})/\lambda}], \\ K_p &= [(\rho_{\mathrm{Au}} - \rho_{\mathrm{Ge}})e^{-(d^p_{\mathrm{Au}} + d_{\mathrm{Pt}})/\lambda}(1 - e^{-d_{\mathrm{Ge}}/\lambda})], \end{aligned} \quad (1)$$

where G is the gravitational constant, $R \sim 50$ μm is the radius of the sphere, K_s (K_p) is a term associated only with the layered structure of the sphere (plate), ρ_s and ρ_{Cr} are the densities of the sapphire sphere and a Cr layer, respec-

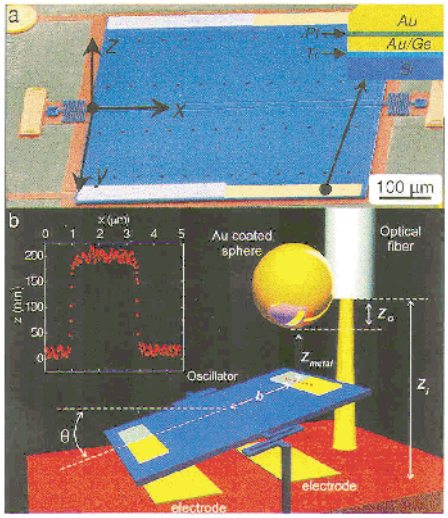

FIG. 1 (color). (a) Scanning electron microscope image of the MTO with the composite sample deposited on it. The coordinate system used in the Letter is indicated. Inset: schematic of the sample deposited on the MTO. The thickness of the different layers are (in order of deposition): $d_{\mathrm{Ti}} = 1$ nm, $d_{\mathrm{Ge}} = 200$ nm, $d_{\mathrm{Pt}} = 1$ nm, and $d^{p}_{\mathrm{Au}} = 150$ nm. The thickness of the layers deposited on the sphere (not shown) are: $d_{\mathrm{Cr}} = 1$ nm and $d^{s}_{\mathrm{Au}} = 200$ nm. (b) Experimental setup. The red dotted line indicates where AFM line cuts were taken. Inset: AFM profile of the sample interface.

tively, and d_i are the thickness of the different layers; see Fig. 1.

A microelectromechanical torsional oscillator (MTO) with a soft spring, $\kappa \sim 10^{-9}$ Nm/rad, and high quality factor, $Q \sim 10^{4}$, has a low coupling with the environment [1,2] and provides a high sensitivity force measurement. The experimental arrangement and calibrations are very similar to those previously used to determine Casimir forces [1,2]. The angular displacement of the MTO, determined by measuring the difference in capacitance between the MTO and the underlying electrodes, $\Delta C = C_{\mathrm{right}} - C_{\mathrm{left}}$, yielded the force acting on it. The sensitivity in the angular deviation is $\delta\theta \simeq 10^{-9}$ rad$/\sqrt{\mathrm{Hz}}$. The films deposited on the sphere and the MTO were characterized by atomic force microscopy (AFM). A typical AFM line cut at the interface between the Au and Ge layers is shown in Fig. 1(b). The observed ridge (a valley in some samples) arises from the imperfect alignment of the mask when depositing the Au and Ge. The AFM images indicate the granular character of the samples, showing a maximum height difference of 22 nm and average lateral dimension of the grains in the 100–150 nm range. The uncertainty in the position of the zero height level (with respect to which the roughness is measured [1]) is ~0.2 nm.

The force sensitivity is improved when the measurements are performed at resonance, $\omega = \omega_r$ [16]. In this case, the minimum detectable force is dominated by thermal fluctuations. Consequently, it is necessary to measure the effect of ΔF_h at resonance. ΔF_h can be described as the product of a function of the separation $e^{-z/\lambda}$ and a function of the x coordinate, the difference in the average mass density. Hence, we changed the separation between the MTO and the sphere as $z_m = z_{mo} + \delta z \cos(\omega_z t)$, with $z_{mo} \gg \delta z$. We simultaneously moved the MTO parallel to the x axis, such that the effective mass density under the sphere was $\rho_{\mathrm{eff}} = \rho^{+} + \rho^{-}\Xi(t)$, where $\rho^{\pm} = (\rho_{\mathrm{Au}} \pm \rho_{\mathrm{Ge}})/2$, and $\Xi(t)$ is a square-wave function with characteristic angular period $T_x = 2\pi\omega_x^{-1}$. At $t = 0$ the sphere is positioned over the MTO on the Au/Au half. By selecting $\omega_z + \omega_x = \omega_r$, ΔF_h has a Fourier component at ω_r given by

$$\mathcal{F}_h(z_{mo}, \omega_r) = \Delta F_h(z_{mo}) \times \frac{2}{\pi} \times I_1\left(\frac{\delta z}{\lambda}\right), \qquad (2)$$

where I_1 is a Bessel function of the second kind. $\mathcal{F}_h(\omega_r)$ is the only Fourier component with a significant signal-to-noise ratio, even though no parts in the system are moving at f_r. We selected $f_x = f_r/70 \sim 10$ Hz. Consequently, $f_z = \omega_z/2\pi = 69 f_x$. The phases of the different signals were chosen to simultaneously cross through 0 every $t_{xr} \equiv 70/f_r (t_{xz} \equiv 69/f_z)$ for the signals at f_x and $f_r(f_z)$. A synthesized signal at f_r, provided by a waveform generator, was used as reference [16]; see Fig. 2(a). The amplitudes were adjusted to provide a peak-to-peak lateral displacement $D \simeq 150$ μm and a vertical amplitude that ranged between $\delta z \simeq 10$ nm at the closest separations to $\delta z \simeq 50$ nm at $z_{mo} = 500$ nm.

For each $T_r = 1/f_r$, ten data points $\mathcal{F}_d(t_i)$ were acquired, $t_i = iT_r/10$, $i = 1, \ldots, 10$. Simultaneously, $\mathcal{P}(t_i) = \mathcal{F}_d(t_i)\cos\omega_r t_i$ and $\mathcal{Q}(t_i) = \mathcal{F}_d(t_i)\sin\omega_r t_i$ were determined. Averaging of $\mathcal{F}_d$, $\mathcal{P}$, and $\mathcal{Q}$ was achieved by adding the signals for all different T_r in the corresponding $i = 1, \ldots, 10$ intervals. Furthermore, the summation over t_i of $\mathcal{P}(t_i)(\mathcal{Q}(t_i))$ yields the in-phase $\mathcal{F}_p$ (quadrature $\mathcal{F}_q$) Fourier component at ω_r.

A strong reduction of the random noise was achieved by increasing the integration time τ. Figure 2 shows the results obtained at a separation $z_{mo} = 300$ nm. Figures 2(b)–2(d) show the observed behavior of $\mathcal{F}_p$ and $\mathcal{F}_q$ in one sample for three characteristic values of τ (the number of repetitions N decreased as τ increased). Figure 2(d) shows the behavior at $\tau = 2000$ s for all seven samples investigated. Several features should be noted in Fig. 2: (i) for each sample and all values of τ, $|\bar{\mathcal{F}}_T| = \sqrt{\bar{\mathcal{F}}_p^2 + \bar{\mathcal{F}}_q^2}$ is constant within the statistical error. $\bar{\mathcal{F}}_p(\bar{\mathcal{F}}_q)$ is the average of $\mathcal{F}_p(\mathcal{F}_q)$ over the different repetitions; (ii) $|\bar{\mathcal{F}}_T|$ remains constant within a factor of 2 for different samples; (iii) the phase $\Theta = \arctan(\bar{\mathcal{F}}_q/\bar{\mathcal{F}}_p)$ takes values close to either 0 or π, indicating that the force is larger over either the Au or the Ge side of the composite sample, respectively. We assume that the forces measured correspond to either $\Theta = 0$ or π [17].

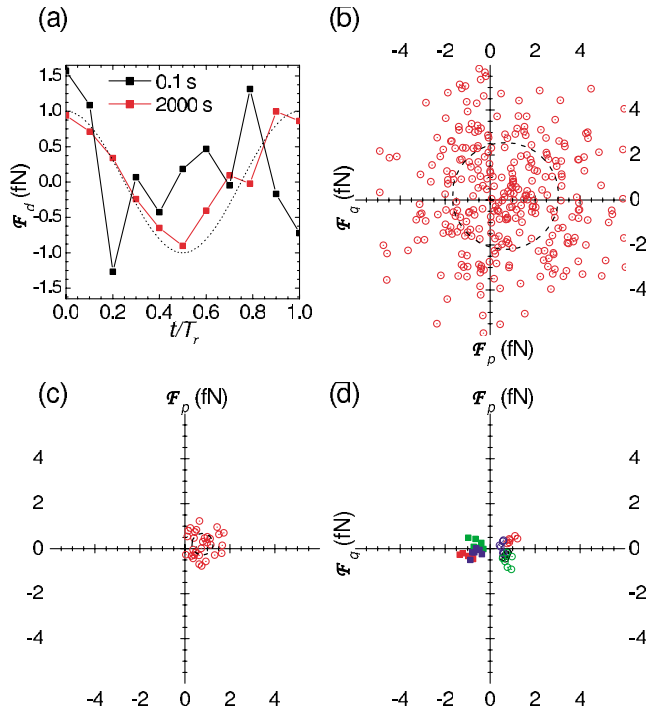

FIG. 2 (color). (a) Dependence of $\mathcal{F}_d(t_i)$ on τ at $z_{mo} = 300$ nm. Data at $\tau = 0.1$ s are scaled by $A = 20$. The dotted line is the reference signal at ω_r, adjusted to fit on the same scale. (b)–(d) $\mathcal{F}_p$ and $\mathcal{F}_q$ at $\tau = 2$ s ($N = 300$), 200 s ($N = 30$), and 2000 s ($N = 6$), respectively. Each point is a repetition of the experiment. The circles in (b) and (c) are centered at $(\bar{\mathcal{F}}_p, \bar{\mathcal{F}}_q)$ and have a radius given by the calculated thermal noise over the relevant τ. The measured noise exceeds the thermal noise by ~20%. (d) Results for all samples. Different symbols and colors have been used for each case.

We obtained the force $\bar{\mathcal{F}}(\tau, z_{mo}) = \bar{\mathcal{F}}_T(\tau, z_{mo}) + s_{N^*}(\tau, z_{mo}) t_{\beta,N^*} \cos\Theta$ required to exclude any Yukawa correction at the $\beta = 95\%$ confidence level. Here, $s_{N^*}(\tau, z_{mo})$ is the mean square error of $\bar{\mathcal{F}}_T(\tau, z_{mo})$, t_{β,N^*} is the Student's coefficient, and $N^* = 6$ is the number of repetitions at $\tau = 2000$ s. Figure 3 shows $\bar{\mathcal{F}}(\tau = 2000\ \text{s}, z_{mo})$ for all samples. Independently of the origin of $\bar{\mathcal{F}}$, the shaded region in Fig. 3 represents values of hypothetical forces *excluded* by our experiment.

Although $\bar{\mathcal{F}} \neq 0$, we do not believe this originates from new physics. Its z_{mo} dependence is not exponential [18]. More importantly, it changes sign depending on the sample under study, showing no correlation with the underlying Au and Ge layers. We attribute $\bar{\mathcal{F}} \neq 0$ to the presence of a different Casimir force arising from z_{mo} taking different values over the Au and Ge sides. With the AFM characterization, the height difference between the two sides is not known to better than $\delta z' \sim 0.1$ nm [19]. This translates into a residual Casimir force difference $|\Delta F_C(200\ \text{nm})| \sim 15$ fN, sufficient to explain the observed $|\bar{\mathcal{F}}(\tau, z_{mo})|$.

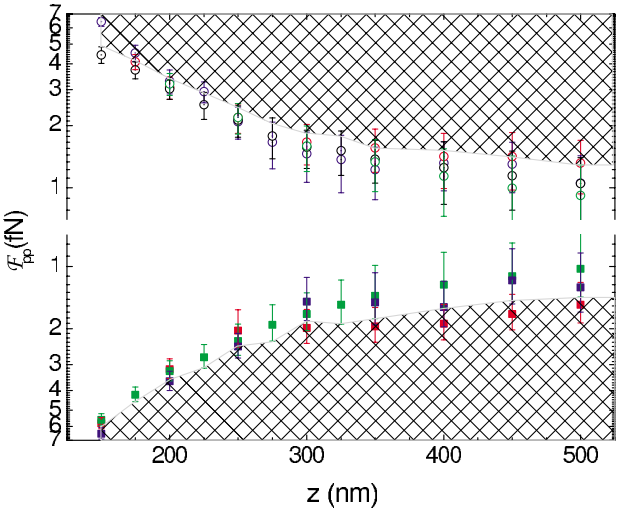

FIG. 3 (color). Dependence of the peak-to-peak $\bar{\mathcal{F}}_T$ on z_{mo}. Colors and symbols are the same as in Fig. 2(d). The shaded regions, representing values of hypothetical forces excluded by our experiments, are defined by the points with minimum absolute value of $\bar{\mathcal{F}}$.

We can, however, rule out other sources for the observed background: (i) a motion of the sphere in a direction not parallel to the MTO's axis was ruled out by performing the experiments without crossing the interface, and at different z_{mo}. The uncertainty $\delta y \sim 3$ nm in the motion of the sphere over the $D = 150$ nm excursion yields a ~0.2 fN error. (ii) Local differences in roughness yield an estimate for the residual force to be $\lesssim 2$ fN, while patch potentials [20] give a contribution $\lesssim 5$ fN. The effect of roughness and patch potentials can be further reduced by moving the sphere back and forth across the interface to points *randomly* selected, with dispersion large enough to average the local changes. This approach yielded the same results. (iii) The effect of the ridge at the interface is also small. A Fourier analysis of its contribution yields $\Phi(200\ \text{nm}) \lesssim 3$ fN. As z_{mo} increases, this contribution decreases rapidly, having a value $\Phi(500\ \text{nm}) \lesssim 0.1$ fN. We note that for samples with a valley instead of a ridge the contribution is negligible. (iv) The finite size of the sample does not affect the Casimir background or the Yukawa corrections. (v) Magnetic or gravitational (Newtonian) forces do not give a measurable background at ω_r. The component of the magnetic force with a signal at ω_r is associated with the preferential presence of magnetic impurities in one of the sides of the engineered sample (either Ge or Au). This force, comparable to the magnetic interaction between isolated atoms, is much smaller than the sensitivity of our apparatus. The Newtonian gravitational force difference between the sphere and the composite Au/Ge sample is $\sim 3 \times 10^{-21}$ N, independent of separation. Hence, it is too small to be detected and it does not have a Fourier component at ω_r.

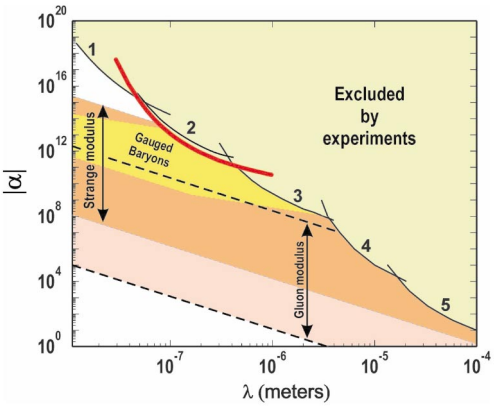

FIG. 4 (color). Values in the $\{\lambda, \alpha\}$ space excluded by experiments. The red curve represents limits obtained in this work. Curves 1 to 5 were obtained by Mohideen's group [7], our group [1], Lamoreaux [6], Kapitulnik's group [8], and Price's group [5], respectively. Also shown are theoretical predictions [21].

The results shown in Fig. 3 can be used to obtain more stringent limits on hypothetical forces. Since the $\Theta = 0$ and $\Theta = \pi$ cases yield very similar absolute values for $\bar{\mathcal{F}}$, at a given z_{mo} we use the smallest $|\bar{\mathcal{F}}(\tau = 2000\ \mathrm{s}, z_{mo})|$ as the maximum $\mathcal{F}_h$. Using Eq. (2), we obtain an $\alpha(\lambda)$ curve. Repeating this procedure for different z_{mo} we obtain a family of curves whose envelope provides the strictest limits arising from our experiments. This curve, together with previous results, is shown in Fig. 4. Our realization of a "Casimir-less" IET yields a $\sim$10-fold improvement (in the $[30, 400]$ nm range) on existing limits for Yukawa-like corrections to Newtonian gravity. This has significant consequences for models of moduli exchange, as proposed by supersymmetry, by further constraining the supersymmetric parameters. We believe that our direct, improved experimental test at submicron separations will continue to motivate theoretical development for this range of separations. We also note that our experiment can be improved by gluing the sphere to the MTO and oscillating the test masses over it. By judiciously designing the test masses, the existing $\delta z'$ can be made to have a different spatial dependence from $\rho_{\mathrm{Au}} - \rho_{\mathrm{Ge}}$. Furthermore, the dominating $\delta z/\lambda$ term from Eq. (2) can be avoided, improving the constraints in $\alpha(\lambda)$. In this scenario, limits on α down to 10^6 could be achieved at separations $z_{mo} \sim 100$ nm.

We are deeply indebted to U. Mohideen for suggesting the randomization of the motion across the interface and for stimulating discussions. R. S. D. acknowledges financial support from the Petroleum Research Foundation through ACS-PRF No. 37542-G. The work of E. F. is supported in part by the U.S. Department of Energy under Contract No. DE-AC02-76ER071428.

*Electronic address: rdecca@iupui.edu

[1] R. S. Decca *et al.*, Phys. Rev. D **68**, 116003 (2003); Ann. Phys. (N.Y.) **318**, 87 (2005).
[2] R. S. Decca *et al.*, Phys. Rev. Lett. **91**, 050402 (2003).
[3] E. Fischbach *et al.*, Phys. Lett. A **318**, 165 (2003); J. C. Long, A. B. Churnside, and J. C. Price, in *The Ninth Marcel Grossmann Meeting*, edited by V. G. Gurzadyan, R. T. Jantzen, and R. Ruffini (World Scientific, Singapore, 2002).
[4] M. Bordag, U. Mohideen, and V. M. Mostepanenko, Phys. Rep. **353**, 1 (2001), and references therein.
[5] J. C. Long, H. W. Chan, and J. C. Price, Nucl. Phys. **B539**, 23 (1999).
[6] S. K. Lamoreaux, Phys. Rev. Lett. **78**, 5 (1997); **81**, 5475(E) (1998).
[7] U. Mohideen and A. Roy, Phys. Rev. Lett. **81**, 4549 (1998); G. L. Klimchitskaya *et al.*, Phys. Rev. A **60**, 3487 (1999); A. Roy and U. Mohideen, Phys. Rev. Lett. **82**, 4380 (1999); B. W. Harris, F. Chen, and U. Mohideen, Phys. Rev. A **62**, 052109 (2000).
[8] J. Chiaverini *et al.*, Phys. Rev. Lett. **90**, 151101 (2003).
[9] G. Bressi *et al.*, Phys. Rev. Lett. **88**, 041804 (2002).
[10] N. Arkani-Hamed, S. Dimopoulos, and G. Dvali, Phys. Lett. B **429**, 263 (1998); Phys. Rev. D **59**, 086004 (1999).
[11] E. G. Adelberger, B. R. Heckel, and A. E. Nelson, Annu. Rev. Nucl. Part. Sci. **53**, 77 (2003).
[12] B. Abbott *et al.*, Phys. Rev. Lett. **86**, 1156 (2001).
[13] H. B. G. Casimir, Proc. K. Ned. Akad. Wet. **51**, 793 (1948).
[14] E. Fischbach *et al.*, Classical Quantum Gravity **18**, 2427 (2001); D. E. Krause and E. Fischbach, Phys. Rev. Lett. **89**, 190406 (2002).
[15] R. Matloob and H. Falinejad, Phys. Rev. A **64**, 042102 (2001). Differences between the model used in this Letter and more sophisticated calculations agree to within 2%, adequate for our order of magnitude estimate.
[16] f_r is a function of the separation due to the nonlinear dependence of the Casimir force [1,2], and it is determined at all z_{mo}.
[17] The deviations of Θ with respect to 0 and π are comparable to those observed when the experiment is replaced by a frequency mixer. We believe that these deviations are electronics induced.
[18] Our experiment does not have enough sensitivity to improve upon existing constraints on power law corrections.
[19] Curvature differences between the MTO and the platform, along the x axis, are smaller than 0.1 nm, the measurement error (WYCO NT3300 optical profilometer). Sample dependent curvatures are a few nm over the 500 μm of the MTO's length.
[20] F. Chen *et al.*, Phys. Rev. A **69**, 022117 (2004).
[21] S. Dimopoulos and A. A. Geraci, Phys. Rev. D **68**, 124021 (2003). Removing the constraints imposed on the undetermined constants $(\lambda^{(0)}/\lambda^{(1)}) \times (M/5 \times 10^{17}\ \mathrm{GeV})$ and $(\lambda_g^{-1}) \times (M/5 \times 10^{17}\ \mathrm{GeV})$ yields the limits on moduli.